

Regulated intramembrane proteolysis of Bri2 (Itm2b) by ADAM10 and SPPL2a/SPPL2b

Lucas Martin, Regina Fluhrer, Karina Reiss, Elisabeth Kremmer, Paul Saftig, Christian Haass

Angaben zur Veröffentlichung / Publication details:

Martin, Lucas, Regina Fluhrer, Karina Reiss, Elisabeth Kremmer, Paul Saftig, and Christian Haass. 2007. "Regulated intramembrane proteolysis of Bri2 (Itm2b) by ADAM10 and SPPL2a/SPPL2b." *Journal of Biological Chemistry* 283 (3): 1644–52.
<https://doi.org/10.1074/jbc.m706661200>.

Nutzungsbedingungen / Terms of use:

licgercopyright

Dieses Dokument wird unter folgenden Bedingungen zur Verfügung gestellt: / This document is made available under these conditions:

Deutsches Urheberrecht

Weitere Informationen finden Sie unter: / For more information see:

<https://www.uni-augsburg.de/de/organisation/bibliothek/publizieren-zitieren-archivieren/publiz/>



Regulated Intramembrane Proteolysis of Bri2 (Itm2b) by ADAM10 and SPPL2a/SPPL2b*

Received for publication, August 10, 2007, and in revised form, October 1, 2007 Published, JBC Papers in Press, October 25, 2007, DOI 10.1074/jbc.M706661200

Lucas Martin^{†1,2}, Regina Fluhrer^{†1}, Karina Reiss[§], Elisabeth Kremmer[¶], Paul Saftig[§], and Christian Haass^{‡3}

From the [†]Center for Integrated Protein Science Munich and the Adolf Butenandt Institute, Department of Biochemistry, Laboratory for Neurodegenerative Disease Research, Ludwig Maximilians University, 80336 Munich, Germany, the [§]Biochemical Institute, University of Kiel, 24098 Kiel, Germany, and [¶]Gesellschaft für Strahlenforschung-Forschungszentrum, Institute for Molecular Immunology, 81377 Munich, Germany

Presenilin, the catalytic component of the γ -secretase complex, type IV prelin peptidases, and signal peptide peptidase (SPP) are the founding members of the family of intramembrane-cleaving GXGD aspartyl proteases. SPP-like (SPPL) proteases, such as SPPL2a, SPPL2b, SPPL2c, and SPPL3, also belong to the GXGD family. In contrast to γ -secretase, for which numerous substrates have been identified, very few *in vivo* substrates are known for SPP and SPPLs. Here we demonstrate that Bri2 (Itm2b), a type II-oriented transmembrane protein associated with familial British and Danish dementia, undergoes regulated intramembrane proteolysis. In addition to the previously described ectodomain processing by furin and related proteases, we now describe that the Bri2 protein, similar to γ -secretase substrates, undergoes an additional cleavage by ADAM10 in its ectodomain. This cleavage releases a soluble variant of Bri2, the BRICHOS domain, which is secreted into the extracellular space. Upon this shedding event, a membrane-bound Bri2 N-terminal fragment remains, which undergoes intramembrane proteolysis to produce an intracellular domain as well as a secreted low molecular weight C-terminal peptide. By expressing all known SPP/SPPL family members as well as their loss of function variants, we demonstrate that selectively SPPL2a and SPPL2b mediate the intramembrane cleavage, whereas neither SPP nor SPPL3 is capable of processing the Bri2 N-terminal fragment.

Regulated intramembrane proteolysis (RIP)⁴ describes a novel cellular mechanism that explains how type I or type II

transmembrane proteins are proteolytically processed (1, 2). RIP is required for reverse signaling and degradation of membrane-retained stubs of certain substrates (1). In a typical example, RIP describes two proteolytic processing steps. First, a large part of the ectodomain is shed and secreted. Subsequently, intramembrane proteolysis cleaves the remaining membrane-bound fragment into two peptides, the intracellular domain (ICD) and a small peptide, which is secreted. Until recently, proteolysis within the membrane was believed to be rather impossible because water molecules, known to be required for hydrolysis of peptide bonds, may have difficulties to penetrate the hydrophobic membrane. However, currently members of three different intramembrane-cleaving protease families are known. All are polytopic proteins with their catalytic sites most likely embedded within their transmembrane domains (1). Intramembrane-cleaving metalloproteases are represented by the site-2 protease (3–5). Site-2 protease (S2P) is required for the regulation of cholesterol and fatty acid biosynthesis via the liberation of the membrane-bound transcription factor sterol regulatory element-binding protein (SREBP) by intramembrane proteolysis. In addition, site-2 protease is also involved in intramembrane processing of ATF6, a protein required for chaperone expression during unfolded protein response. Prior to intramembrane cleavage, both substrates are first shed by a luminal cleavage via site-1 protease (6).

Intramembrane-cleaving serine proteases are represented by the growing family of rhomboids. At least *Drosophila* rhomboids are known to be involved in intramembrane proteolysis of Spitz, Gurken, and Keren. Their cleavage is required for epidermal growth factor receptor signaling (7–9), but an initiating shedding event is apparently not required. Rhomboids are the first intramembrane-cleaving proteases for which crystal structures could be resolved (10–14). The crystal structures suggest that their catalytically active Ser-His dyad and water molecules are indeed embedded within the interior of the membrane.

The family of intramembrane-cleaving aspartyl proteases is represented by γ -secretase, the signal peptide peptidase (SPP) (15), its homologues the SPP-like (SPPL) proteases (1, 16–18), and the bacterial type IV prelin peptidases, which cleave very close to or right at the membrane (19).

* This work was supported in part by the Leibniz Award of Deutsche Forschungsgemeinschaft (to C. H.), Deutsche Forschungsgemeinschaft Grant HA1737-11-1 (to C. H. and R. F.), Sonderforschungsprogramm Grants SFB 415 (to P. S. and K. R.) and SFB 596 (to C. H. and E. K.), and the Center for Integrated Protein Science Munich. The costs of publication of this article were defrayed in part by the payment of page charges. This article must therefore be hereby marked "advertisement" in accordance with 18 U.S.C. Section 1734 solely to indicate this fact.

[†] Both authors contributed equally to this work.

² Member of the Elitenetzwerk Bayern Graduate Program "Protein Dynamics in Health and Disease."

³ Supported by a "Forschungsprofessur" grant from the Ludwig Maximilians University. To whom correspondence should be addressed. E-mail: chaass@med.uni-muenchen.de.

⁴ The abbreviations used are: RIP, regulated intramembrane proteolysis; Bri2, British dementia protein-2; Itm2b, integral membrane protein 2b; ABri, amyloid British dementia protein; ICD, intracellular domain; NTF, N-terminal fragment; ADAM, a disintegrin and metalloprotease; (Z-LL)₂-ketone, 1, 3-di-(N-benzyloxycarbonyl-L-leucyl-L-leucyl)aminoacetone; DAPT, N-[N-(3,5-difluorophenacetyl)-L-alanyl]-S-phenylglycine t-butyl ester; SPP,

signal peptide peptidase; SPPL, SPP-like; ER, endoplasmic reticulum; TNF α , tumor necrosis factor α ; siRNA, small interfering RNA; HEK, human embryonic kidney; BFA, brefeldin A; HA, hemagglutinin.

γ -Secretase is a complex composed of presenilin-1 or presenilin-2, nicastrin, APH-1 (anterior pharynx defective-1), and PEN-2 (presenilin enhancer-2) (20). Presenilin is the catalytically active component of the γ -secretase complex (21) and contains the GXGD protease active site motif (22). γ -Secretase cleaves numerous type I substrates including Notch and the β -amyloid precursor protein (20, 23, 24). In both cases, the ICDs of the substrates are released to the cytosol. Although the Notch ICD is required for reverse signaling, a functional role of the β -amyloid precursor protein ICD is currently under debate (20, 24), and for a number of other substrates the function of the ICD is unknown. Besides the ICDs, γ -secretase also liberates the amyloid β -peptide and the corresponding Notch β -peptide (25). Amyloid β -peptide accumulates in amyloid plaques and vascular deposits characteristic for Alzheimer disease. Although γ -secretase only accepts type I-oriented substrates, members of the SPP family are required for intramembrane proteolysis of type II transmembrane proteins (1). SPP family members are differentially located within the cells (26, 27). SPP and SPPL3 are predominantly observed within the endoplasmic reticulum (ER)/Golgi, whereas SPPL2a and SPPL2b are additionally found in late Golgi compartments and endosomes/lysosomes (26). Consistent with its subcellular localization, SPP is required for the removal of signal peptides from the ER membrane (15). Beside its function in removal of signal peptides, SPP is also involved in immune surveillance and intramembrane cleavage of the hepatitis C viral core protein (15, 28). No substrate has so far been identified for the ER/Golgi located SPPL3. For SPPL2a and SPPL2b currently two *in vivo* substrates, tumor necrosis factor α (TNF α) and the Fas ligand, are known (27, 29, 30).

The ectodomains of both substrates undergo shedding by members of the ADAM (a disintegrin and metalloprotease) family. TNF α is further processed by intramembrane cleavages of SPPL2a/SPPL2b to produce the TNF α ICD and the secreted TNF α C domain (29). The TNF α ICD triggers expression of the pro-inflammatory cytokine interleukin-12 in dendritic cells (27). Because of the restricted cell and tissue specific expression of TNF α and FasL, additional substrates for SPPL2a/SPPL2b are to be expected.

We therefore investigated the type II-oriented transmembrane protein Bri2, also known as Itm2b, which is the precursor of the ABri amyloid protein (31). For clarity, we will use the term Bri2 throughout the manuscript. Bri2 undergoes processing by furin and related proteases within its ectodomain (32, 33), which leads to the release of its 4-kDa C-terminal propeptide. Mutations of the stop codon in the *bri2* (*itm2b*) gene are responsible for the generation of a longer open reading frame, therefore causing the release of a longer propeptide by furin-mediated proteolysis (31–33). The mutant Bri2 amyloid propeptides (ABri) tend to aggregate into oligomers, protofibrils, and further into amyloid deposits and cause familial British (31) and Danish dementia (34), which are autosomal dominant neurodegenerative diseases characterized by amyloid angiopathy, plaques, and neurofibrillar tangles (33, 35).

We have now investigated the proteolytic processing of Bri2. Surprisingly, in addition to the furin-mediated release of the C-terminal propeptide, a large part of the remaining ectodo-

main, the so-called BRICHOS domain, is shed by ADAM10 and released to the extracellular space. The remaining membrane-associated N-terminal fragment (NTF) undergoes intramembrane proteolysis mediated by SPPL2a or SPPL2b. This cleavage generates the Bri2 ICD, which is liberated into the cytosol and the secreted Bri2 C domain.

EXPERIMENTAL PROCEDURES

Cell Culture, cDNAs, and Transfection—HEK293EBNA, HEK293TR, and SH-SY5Y cells were cultured in Dulbecco's modified Eagle's medium with Glutamax (Invitrogen) supplemented with 10% fetal calf serum (Invitrogen) and 1% penicillin/streptomycin (Invitrogen). SNKBE cells were cultured in Ham's F-12 medium (Cambrex Bio Science, Verviers, Belgium) supplemented with 2.5% non-essential amino acids (Invitrogen) and 10% fetal calf serum. A-431 cells were cultured in Advanced RPMI 1640 medium (Invitrogen) supplemented with 0.5% penicillin/streptomycin and 10% fetal calf serum. Using PCR, a C-terminal HA tag (AYPYDVPDYA) was added to all constructs. SPPL2a, SPPL2a D412A, SPPL2b, SPPL2b D421A, and SPPL3 D272A were subcloned into the *NheI* and *NotI* or *EcoRI* and *XhoI* sites of pcDNA 3.1. Zeo[−] (Invitrogen) and stably transfected into HEK293EBNA cells. SPP, SPP D265A, and SPPL3 were subcloned into the *EcoRI* and *XhoI* sites of pcDNA 4/TO A (Invitrogen) and stably transfected into HEK293 TR cells (Invitrogen). Transfection of cells was carried out using Lipofectamine 2000 (Invitrogen) according to the manufacturer's instructions, and single cell clones were generated by selection in 200 μ g/ml zeocine (Invitrogen). To induce expression of SPP, SPP D265A, and SPPL3, cells were incubated with 1 μ g/ml doxycycline (BD Biosciences) added to the cell culture medium for at least 48 h.

Bri2 cDNA was purchased from RZPD (Deutsches Ressourcenzentrum für Genomforschung, Berlin, Germany). After the starting methionine an N-terminal FLAG tag (DYKDDDDK) and, at the C terminus of the protein, a V5 tag (GKPIPNLLGLDST) were added, and the PCR product was subcloned into the *HindIII* and *XbaI* sites of pcDNA6.0-V5-His A (Invitrogen). The Bri2 Δ E and the Bri2 Δ FC constructs were generated by deleting the C-terminal part of the protein after amino acids 94 and 240, respectively. The Bri2 KR 243/244 AA (KR/AA) construct was generated by PCR mutagenesis. These Bri2 constructs also contain an N-terminal FLAG tag and a C-terminal V5 tag and were subcloned into the *HindIII* and *XbaI* sites of pcDNA6.0-V5-His A (Invitrogen). All cDNA constructs were sequenced for verification. Bri2 cDNAs were either transiently or stably expressed in cell lines stably expressing SPPs or SPPLs as described above.

Antibodies, Immunoprecipitation, and Immunoblotting—The anti-HA peroxidase-coupled 3F10 antibody was obtained from Roche Diagnostics. The monoclonal anti-FLAG M2 and the polyclonal HA 6908 antibody were obtained from Sigma. Polyclonal and monoclonal V5 antibodies were purchased from Chemicon (Schwalbach, Germany) and Invitrogen, respectively. The polyclonal antibodies against ADAM10, Calnexin, and ADAM17 (TACE) were purchased from Calbiochem, Stressgene/Biomol (Hamburg, Germany), and Oncogene, respectively. The polyclonal anti-Bri2 antibody (ITM2b

Regulated Intramembrane Proteolysis of Bri2

ab14307) directed against the first 60 amino acids of human Bri2 was obtained from Abcam (Cambridge, UK). The monoclonal SPPL2b-specific antibody CADG-3F9 directed against amino acids 518–535 of the protein was established by Dr. Elisabeth Kremmer (GSF-Forschungszentrum, Munich). Anti-mouse, anti-rabbit, and anti-chicken peroxidase secondary antibodies were purchased from Promega (Madison). Immunoprecipitation assays, gel electrophoresis, immunoblotting experiments, and co-immunoprecipitation assays were carried out as described previously (26, 29).

Immunocytochemistry and Confocal Imaging—The indicated cell lines were grown on polylysine-coated glass coverslips to 50–80% confluence and processed for immunofluorescence as described before (26). Confocal images were obtained with Zeiss 510Meta confocal laser scanning microscope system equipped with a 100/1.3 objective described previously (36). Images were assembled and processed using Adobe Illustrator.

Inhibitor Treatment and RNA Interference—To inhibit SPPL2b, cells were treated overnight with a final concentration of 15 μ M (Z-LL)₂-ketone (Calbiochem), a known SPP inhibitor (37). As a control, cells were treated with 3 μ M γ -secretase inhibitor DAPT (38) or the respective carrier.

To block specific metalloprotease activities, cells were grown in a 6-well format and treated overnight with either 50 μ M TAPI-1 (Peptides International) or 50 μ M TAPI-2 (Peptides International). Hydroxamate-based inhibitors GW280264 (5 μ M) and GI254023 (5 μ M) are described elsewhere (39).

For quantification, proteins were immunoblotted as described above and detected using the enhanced chemiluminescence technique (GE Healthcare). The chemiluminescence signals of at least three independent experiments were measured with a CD camera-based imaging system (Alpha-Innotec, Kasendorf, Germany). Statistical significance was determined with Student's *t* test. Statistically significant *p* values of <0.05 or <0.005 are represented by or, respectively.

RNA interference experiments were carried out as follows. 1×10^6 cells/well were plated in a polylysine-coated 6-well format. After a 2-h incubation, cells were transfected with the indicated small interfering RNA (siRNA) (Dharmacon siRNA SMARTpools: catalog numbers M-0040503-01 (ADAM10), M-003453-00 (ADAM17), and D-001206-13 (non-targeting control)), using Lipofectamine 2000 (Invitrogen) according to the manufacturer's instructions. 24 h after transfection, the medium was exchanged, and cells were harvested 48 h after transfection. Five independent experiments were quantified as described above. BRICHOS and Bri2 Δ FC levels were first normalized to the calnexin expression level, and then the ratio of BRICHOS to Bri2 Δ FC was determined. Resulting data for control siRNA were set to 100%.

Where indicated cells were treated overnight with 10 μ g/ml brefeldin A (BFA; Sigma-Aldrich). As a control, cells were incubated with the respective carrier.

RESULTS

Shedding of Bri2 by ADAM10—The Bri2 protein is a type II transmembrane protein, known to be processed within its ectodomain by furin and related proteases (Fig. 1A, *proBri2*) (32, 33, 40). Consequently, a membrane-bound fragment, con-

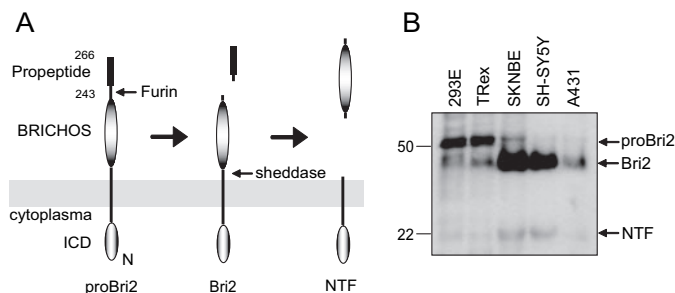


FIGURE 1. Proteolytic processing of Bri2. A, schematic presentation of Bri2 processing by furin (or related proteases) and a sheddase. B, proteolytic processing of endogenous Bri2. Membrane preparations of human embryonic kidney cells (HEK293/TRex), SKNBE cells, SH-SY5Y cells, and A431 cells were analyzed using the anti-Bri2 antibody (ITM2b ab14307) directed against the first 60 amino acids of human Bri2. Besides the expected Bri2 variants (*proBri2*/Bri2), an additional Bri2 NTF of ~22 kDa was detected in all cell lines.

taining the so-called BRICHOS domain, remains after this initial processing (Fig. 1A, *Bri2*). As expected, Bri2 containing the propeptide (*proBri2*) was detected at a molecular mass of ~50 kDa in all cell lines tested. The mature Bri2 variant lacking the propeptide (*Bri2*) was detected at a slightly lower molecular weight and was most prominently visible in cell lines of neuronal origin (Fig. 1B, *SKNBE*, *SH-SY5Y*). However, besides these expected Bri2 species, we additionally detected a lower molecular mass Bri2 NTF of ~22 kDa in all cell lines investigated (Fig. 1B). We therefore assumed that Bri2 might undergo shedding because such a proteolytic processing step would result in the generation of a small membrane retained stub (Fig. 1A, *NTF*).

If such a shedding event takes place, one would expect a secreted counterpart containing the BRICHOS domain (see Fig. 1A). To allow identification of such a secreted domain, we inserted a V5 tag directly at the C terminus of the BRICHOS domain generating Bri2 Δ FC (Fig. 2A). Upon expression of this cDNA construct, we indeed detected the ~25-kDa BRICHOS domain as a secreted species in the conditioned medium (Fig. 2B). Similar to cells expressing endogenous Bri2 (Fig. 1B), NTF was observed within the cell lysate (Fig. 2B). This suggests that the BRICHOS domain and the Bri2 NTF are generated by a novel shedding event of Bri2 and may explain the observation of a N-terminal Bri2 fragment of unknown origin by Choi *et al.* (40). In analogy to many γ -secretase substrates, which require shedding by proteases of the ADAM family, we investigated whether a member of this protease family is involved in shedding of Bri2. Broad ADAM protease inhibitors, such as TAPI-1 and TAPI-2 (41), strongly reduced the secretion of the BRICHOS domain (Fig. 2C). The nature of the metalloprotease activity was narrowed down using two hydroxamate-based inhibitors that differ in their inhibitory profile. The inhibitor GW280264X has been shown to block ADAM17 and ADAM10, whereas the compound GI254023X preferentially blocks ADAM10 (39). Both inhibitors strongly blocked secretion of the BRICHOS domain (Fig. 2D). To finally determine which of the two proteases is required for shedding of Bri2, we selectively knocked down ADAM10 and ADAM17 using RNA interference techniques. Upon transient knockdown of ADAM10, secretion of the BRICHOS domain was significantly reduced compared with cells treated with a control RNA interference oligonucleotide. The knockdown of ADAM17 on the

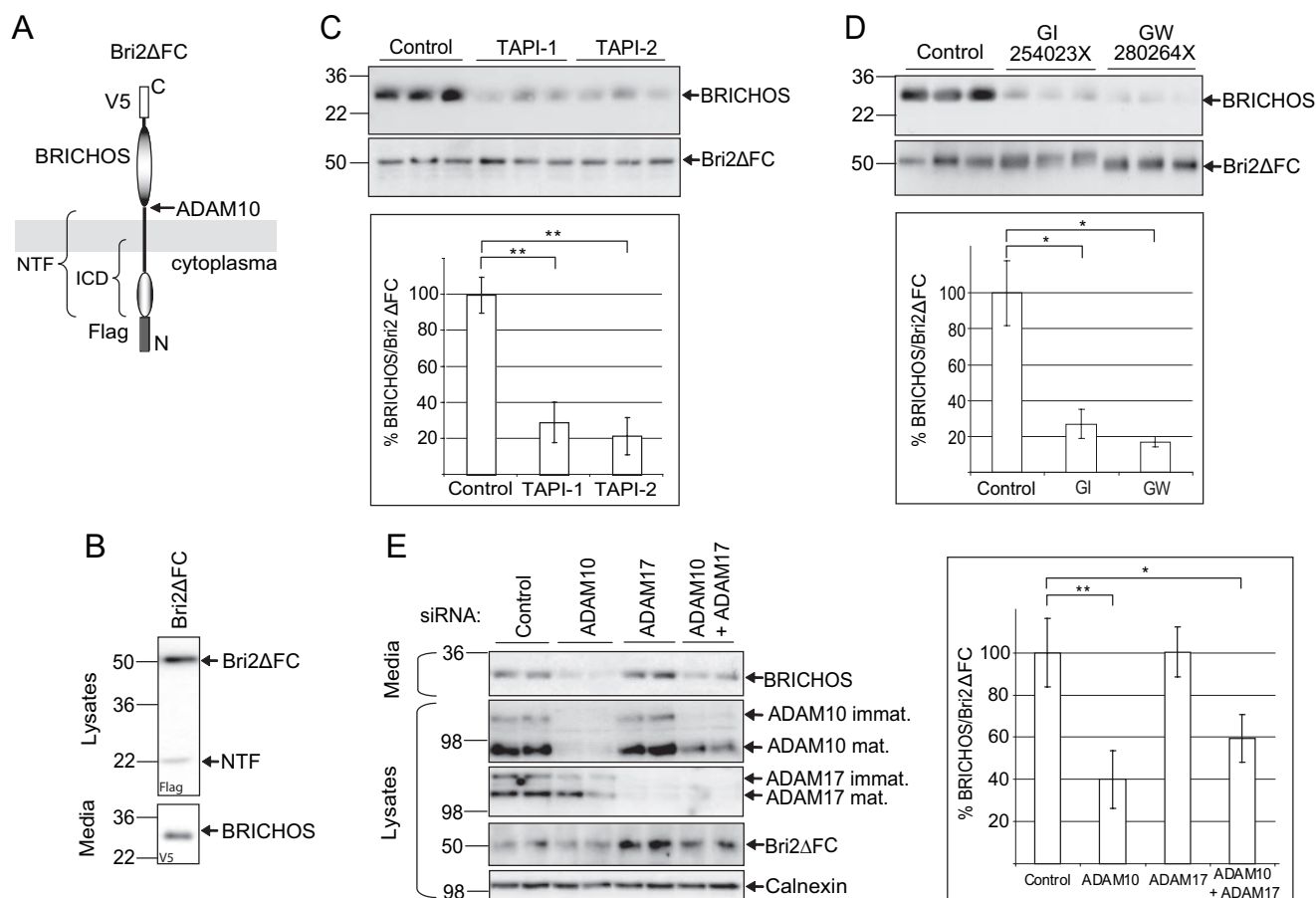


FIGURE 2. Shedding of Bri2 by ADAM10. *A*, schematic presentation of Bri2 Δ FC. Bri2 Δ FC lacks the C-terminal propeptide. The V5 tag was inserted at amino acid 240 of Bri2. *B*, proteolytic processing of Bri2 Δ FC. Cell lysates and the conditioned medium of HEK293 cells stably expressing Bri2 Δ FC were analyzed for the indicated processing products. Bri2 Δ FC was detected as a single band of ~ 50 kDa using the anti-FLAG antibody. In addition the above described (Fig. 1*B*) NTF of ~ 22 -kDa was detected in the cell lysate. The potentially *N*-glycosylated BRICHOS domain was observed in the conditioned medium as an ~ 25 -kDa peptide using the V5 antibody. *C*, TAPI treatment reduces BRICHOS secretion. HEK293 cells stably expressing Bri2 Δ FC were treated with 50 μ M TAPI-1 or TAPI-2 overnight. Control cells were treated with carrier (Me₂SO) only. Compared with controls, cells treated with the TAPI-1 and TAPI-2 show a significantly reduced ($71 \pm 11.2\%$, $p < 0.001$, and $78 \pm 10.2\%$, $p < 0.001$, respectively) BRICHOS secretion. Detection of Bri2 Δ FC was used as a loading control (*lower panel*). *D*, selective ADAM10/ADAM17 inhibitors reduce BRICHOS secretion. HEK293 cells stably expressing Bri2 Δ FC were treated with 5 μ M ADAM10 or ADAM10- and ADAM17-specific inhibitor GI254023X or GW280264X, respectively, overnight. GI254023X and GW280264X cause a significantly reduced liberation of the BRICHOS domain ($73 \pm 8\%$, $p < 0.010$, and $83 \pm 3\%$, $p < 0.015$, respectively). *E*, ADAM10 is the BRICHOS sheddase. HEK293 cells stably expressing Bri2 Δ FC were transfected with specific siRNA against ADAM10, ADAM17, or a nonspecific siRNA as a control. Knockdown efficiency was proven by immunoblotting for ADAM10 and ADAM17. Detection of calnexin serves as a loading control. BRICHOS liberation was strongly reduced upon knockdown of ADAM10 or both ADAM10 and ADAM17 ($60 \pm 13\%$, $p < 0.001$, and $40 \pm 11\%$, $p < 0.017$, respectively). Knockdown of ADAM17 alone does not reduce the secretion of the BRICHOS domain, indicating that ADAM10 is the major Bri2 sheddase. Note that the knockdown efficiency of ADAM10 in double knockdown experiments is slightly reduced, allowing a stronger BRICHOS secretion compared with the single ADAM10 knockdown.

other hand did not have a significant effect on the secretion of the BRICHOS domain. A combined knockdown of ADAM10 and ADAM17 failed to further reduce BRICHOS secretion (Fig. 2*E*). Taken together, these data demonstrate that Bri2 undergoes ectodomain shedding via proteolytic processing by ADAM10.

Bri2 Is a Substrate for Intramembrane Proteolysis by SPPL2a and SPPL2b—Ectodomain shedding produces membrane-retained stubs that frequently undergo additional processing within their transmembrane domains to either remove the membrane-bound stub or to induce nuclear signaling (see Introduction). To investigate whether Bri2 is also a substrate for intramembrane proteolysis, we expressed the full-length pro-Bri2 protein in HEK293 cells and investigated the proteolytic processing by an immunoprecipitation analysis (Fig. 3*B*). Interestingly, in addition to pro-Bri2, Bri2, and NTF, we

detected a fragment of ~ 10 kDa (ICD) in the cell lysate (Fig. 3*B*) suggesting that the NTF may be further processed. Importantly, NTF and ICD generation occurs via processing by endogenous proteases, and the Bri2 substrate has not been modified at any cleavage site. ICD generation suggests that Bri2 undergoes proteolysis by an intramembrane-cleaving protease. Because Bri2 is a type II-oriented protein, obvious candidates for intramembrane proteolysis are the members of the SPP/SPPL family. To determine whether any of the SPP family members could mediate intramembrane proteolysis of Bri2, we co-expressed SPP, SPPL2a, SPPL2b, and SPPL3 with the full-length Bri2 protein in HEK293 cells. In addition, the catalytically inactive variants with the corresponding TM7 aspartate mutated to alanine (D/A mutants) (26) were also investigated. The pro-Bri2 protein was expressed with a C-terminal V5 tag and an N-terminal FLAG tag to allow detection of

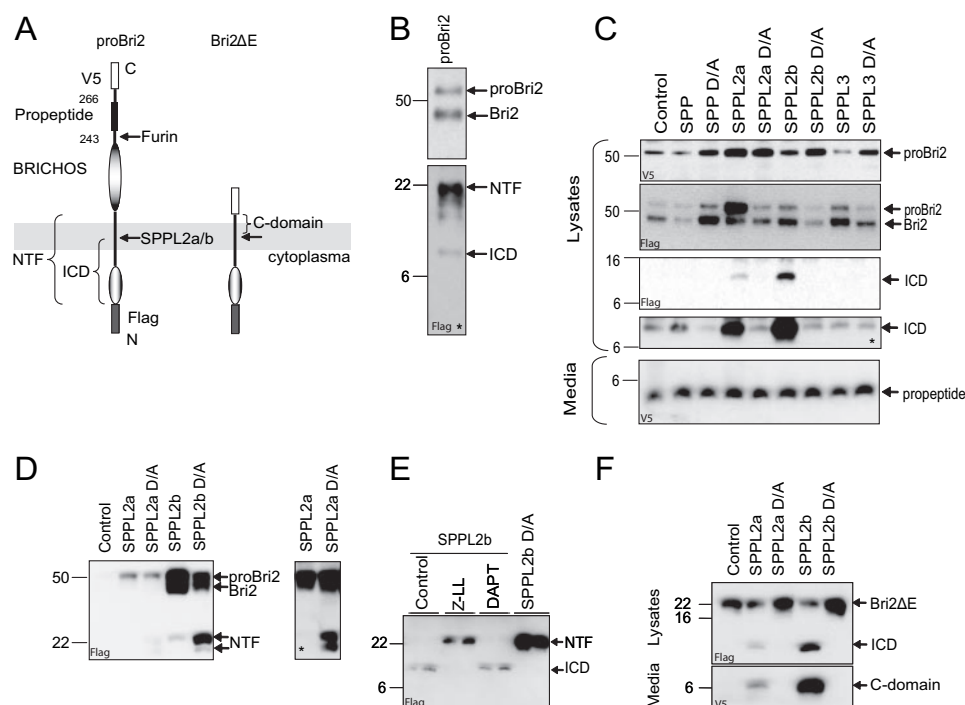


FIGURE 3. Bri2 is a substrate for intramembrane proteolysis by SPPL2a and SPPL2b. *A*, schematic presentation of pro-Bri2 and Bri2 Δ E. Bri2 constructs are N-terminally FLAG-tagged and C-terminally V5-tagged. The Bri2 Δ E construct lacks the BRICHOS ectodomain and the propeptide. *B*, detection of a 10-kDa N-terminal intracellular fragment. Pro-Bri2 was stably overexpressed in HEK293 cells. Cell lysates were immunoprecipitated using the anti-FLAG antibody and were subjected to SDS-PAGE and Western blot analysis. As described in the legends for Figs. 1*B* and 2*B*, a NTF of \sim 22 kDa was detected. In addition, another intracellular fragment of about 10 kDa (ICD) was detected after longer exposure. Note that the proteolytic products of Bri2 (NTF, ICD; mature Bri2) were generated by endogenous proteases. *C*, proteolytic processing of Bri2 by SPPL2a and SPPL2b. HEK293 cells stably expressing SPP, SPPL2a, SPPL2b, and SPPL3, or the respective catalytically inactive D/A mutants were transiently transfected with pro-Bri2. Cell lysates and the conditioned media were immunoprecipitated using antibodies against the FLAG tag and the V5 tag, respectively, and were subsequently subjected to SDS-PAGE and Western blot analysis. The indicated Bri2 fragments were detected using antibodies against the indicated tags. In all cell lines, the propeptide was secreted into the conditioned medium. Using an antibody against the C-terminal V5 tag, pro-Bri2 was detected as a single band in the cell lysates, whereas pro-Bri2 and the furin-processed mature Bri2 were detected as a double band with an antibody directed against the N-terminal FLAG tag. An additional \sim 10-kDa anti-FLAG positive band (Bri2 ICD) was detected in cells expressing SPPL2a or SPPL2b but not in cells expressing SPP, SPPL3, or the catalytically inactive mutants. Upon longer exposure, the endogenously produced ICD was also detected as shown in *B*. *D*, co-immunoprecipitation of Bri2 and SPPL2a/SPPL2b. HEK293 cells expressing SPPL2a/SPPL2b or the inactive mutants SPPL2a/SPPL2b D/A were transiently transfected with pro-Bri2. Immunoprecipitation of SPPL2a or SPPL2b, using an anti-HA antibody, and detection of Bri2, using an anti-FLAG antibody, revealed binding of pro-Bri2, Bri2, and the Bri2 NTF to SPPL2a (longer exposure) and SPPL2b. *E*, pharmacological inhibition of SPPL2b prevents Bri2 ICD generation. HEK293 cells stably expressing the indicated SPPL variants and pro-Bri2 were treated as indicated with 15 μ M (Z-LL) $_2$ -ketone or 3 μ M DAPT overnight. Control cells were treated with Me $_2$ SO. Bri2 ICD formation was inhibited by the SPP/SPPL-specific inhibitor (Z-LL) $_2$ -ketone but not by the γ -secretase inhibitor DAPT. Note the accumulation of the NTF upon (Z-LL) $_2$ -ketone treatment and expression of catalytically inactive SPPL2b variant (SPPL2b D/A). *F*, proteolytic processing of Bri2 Δ E by SPPL2a and SPPL2b. HEK293 cells stably expressing the indicated SPPL variants were transiently transfected with Bri2 Δ E. Cell lysates and conditioned media were analyzed for Bri2-specific fragments using antibodies against the FLAG tag and the V5 tag, respectively. The Bri2 Δ E construct was processed by SPPL2a and SPPL2b, giving rise to the Bri2 ICD and a secreted C domain. The catalytically inactive mutants do not process Bri2 Δ E and fail to generate the ICD and the C domain.

proteolytic processing products from both ends (Fig. 3*A*). Consistent with previous findings, the prodomain of Bri2 is proteolytically removed (32, 33). Immunoblotting of cell lysates with an antibody to the N-terminal FLAG tag revealed both Bri2, lacking the C-terminal propeptide, and pro-Bri2 still containing the propeptide (Fig. 3*C*). In contrast, the antibody to the C-terminal V5 tag selectively detects pro-Bri2 in the cell lysate (Fig. 3*C*, upper panel). In addition, the tagged 5-kDa propeptide was found to be released and secreted into the media of all cell lines (Fig. 3*C*). Removal of the prodomain occurs independently of whether and which SPP/SPPL was expressed or

not (Fig. 3*C*). Robust amounts of the 10-kDa N-terminal fragment corresponding to the ICD of Bri2 were detected in cell lysates only upon expression of SPPL2a and SPPL2b (Fig. 3*C*). In contrast, no increase in ICD generation above the background level was detectable upon expression of SPP or SPPL3 (Fig. 3*C*). Increased amount of ICD was only produced in the presence of catalytically active SPPL2a/SPPL2b, and its production was abolished upon expression of the catalytically inactive D/A mutants of SPPL2a and SPPL2b (Fig. 3*C*). Note that longer exposure reveals the ICD generated by endogenous processing (compare Fig. 3, *B* and *C*). We concluded that this fragment might be produced via intramembrane proteolysis by SPPL2a and SPPL2b, and therefore we investigated whether SPPL2a/SPPL2b may directly interact with the Bri2 substrate. Co-immunoprecipitation allowed the co-isolation of the 22-kDa NTF as well as of the furin-generated Bri2 protein and the full-length pro-Bri2 together with SPPL2a/SPPL2b (Fig. 3*D*). NTF co-immunoprecipitated at high levels when the inactive D/A mutation of SPPL2a or SPPL2b was co-expressed (Fig. 3*D*), which is similar to the accumulating C-terminal fragments of γ -secretase substrates upon its inhibition (42). In line with these findings, the NTF accumulated upon treatment with (Z-LL) $_2$ -ketone, a selective SPP/SPPL inhibitor (15), but not with the γ -secretase inhibitor DAPT (38). Furthermore, (Z-LL) $_2$ -ketone inhibits ICD generation, as does expression of the catalytically inactive SPPL2b D/A mutant (Fig. 3*E*).

To prove whether Bri2 lacking its ectodomain is sufficient for SPPL2 cleavage, we generated a recombinant Bri2 NTF (Fig. 3*A*, Bri2 Δ E) corresponding to the Notch Δ E construct previously used to investigate γ -secretase function (43). Expression of this construct was sufficient to allow SPPL2a/SPPL2b-dependent ICD formation of Bri2 (Fig. 3*F*). Moreover, in the conditioned medium of cells expressing Bri2 Δ E, we detected the secreted counterpart of the ICD, which we called Bri2 C domain (Fig. 3, *A* and *F*). Both, ICD and C domain generation are blocked upon expression of the D/A mutants of SPPL2a/SPPL2b (Fig. 3*F*).

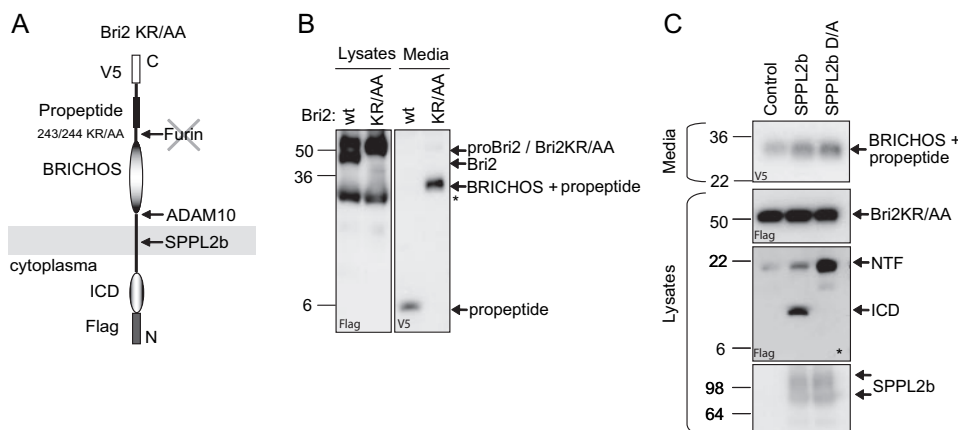


FIGURE 4. Shedding by ADAM10 and intramembrane cleavage by SPPL2b occur independently of a prior cleavage of Bri2 by furin. *A*, schematic presentation of Bri2KR/AA. The residues Lys-243 and Arg-244 were both mutated to alanine, resulting in a furin-uncleavable Bri2 variant. *B*, Bri2KR/AA was not processed by furin. Cells stably expressing the indicated Bri2 variants were analyzed for the indicated cleavage products as described in the legend to Fig. 3C. In cell lines expressing Bri2KR/AA, the BRICHOS domain containing the uncleaved propeptide was secreted into the conditioned medium, whereas no liberated propeptide was detected. In cell lines expressing wild-type (wt) Bri2, the secreted BRICHOS domain was not detected because the V5 tag was removed by furin-mediated processing. In cell lysates, Bri2KR/AA was detected as a single protein of ~50 kDa, indicating that Bri2KR/AA cannot be processed by furin. *C*, Bri2KR/AA was processed by SPPL2b and ADAM10. Cells stably expressing the indicated SPPL2b variants and Bri2KR/AA were analyzed for the indicated processing products as described in the legend to Fig. 3C. In all cell lines, the BRICHOS domain containing the uncleaved propeptide was secreted into the conditioned media. In cells expressing the active SPPL2b, the Bri ICD (10 kDa) was detected additionally. Asterisk indicates longer blot exposure.

Shedding by ADAM10 and Intramembrane Cleavage by SPPL2b Occur Independently of a Prior Cleavage of Bri2 by Furin—Next, we investigated whether shedding of Bri2 by ADAM10 requires a previous cut by furin. Therefore we blocked the furin cleavage of Bri2 by mutagenizing the corresponding cleavage site at amino acid 243/244 (33) generating Bri2KR/AA (Fig. 4A). In cells expressing the mutant Bri2KR/AA protein, no propeptide was detected in the conditioned medium, but an ~30-kDa fragment corresponding to a peptide containing the BRICHOS domain and the propeptide was observed (Fig. 4B). In the corresponding lysates, only one single band representing the FL Bri2KR/AA protein was detected (Fig. 4B), confirming that propeptide cleavage was abolished in the mutant Bri2 variant. The mutant Bri2 substrate was then co-expressed with SPPL2b and the inactive SPPL2b D/A mutant (Fig. 4C). Secretion of the BRICHOS domain (including the propeptide) was independent of the biological activity of SPPL2b (Fig. 4C). Thus these data demonstrate that shedding of Bri2 by ADAM10 occurs independent of furin-mediated processing. Moreover, furin-mediated processing of Bri2 was not required for its subsequent intramembrane proteolysis by SPPL2b as demonstrated by the ICD generation in Fig. 4C. This was also supported by the accumulation of the Bri2 NTF upon expression of the catalytically inactive SPPLb D/A mutant (Fig. 4C).

Subcellular Localization of Bri2 and SPPL2b—The above described results demonstrate that preferentially SPPL2a and SPPL2b process Bri2. To investigate in which cellular compartment Bri2 and SPPL2b interact, we performed immunocytochemical experiments. Bri2 and SPPL2b co-localize within a vesicular structure close to the nucleus (Fig. 5A). Co-localization studies using antibodies against the V5 or HA tag (for Bri2 or SPPL2b, respectively) and Giantin revealed that the

protease and its substrate are both co-expressed within the Golgi (Fig. 5A). Additional co-staining within later secretory compartments, like endosomes, cannot be excluded. This suggests that proteolytic processing of Bri2 may be initiated upon its arrival in the Golgi. However, co-localization by itself is not sufficient for RIP of Bri2. This is demonstrated by BFA treatment that blocks forward transport from the ER to the Golgi (44). Under these conditions, SPPL2b and Bri2 fully co-localize within an ER/Golgi fusion compartment (Fig. 5B). Interestingly, the co-localization under these conditions does not allow processing of Bri2 by SPPL2b because production of the Bri2 ICD is blocked (Fig. 5C). Consistent with previous findings, furin-mediated processing was also abrogated under these conditions (40) as demonstrated by the accumulation of pro-Bri2 in the cell lysate (Fig. 5, C and D). Upon BFA treatment, we were also not able to detect the propeptide in either the medium or the corresponding lysate (Fig. 5D). In addition, BFA treatment of cells expressing Bri2ΔFC (see Fig. 2A) reduced the secretion of the BRICHOS domain below the detection level, and the BRICHOS domain was also not detected in the corresponding lysate (Fig. 5E). Taken together, these data suggest that co-localization of Bri2 with its proteases alone is not sufficient for RIP of Bri2.

DISCUSSION

We have demonstrated that Bri2 is a novel substrate for RIP. In contrast to previous knowledge, we could demonstrate that Bri2 is processed not only by furin or related proteases but also by ADAM10 and SPPL2a/SPPL2b (Fig. 6). The ADAM10 cleavage liberates the BRICHOS domain, which, like the ectodomains of many other proteins, is secreted. The function of the BRICHOS domain is unclear (45). Interestingly, the Bri2 homologues, Bri1 and Bri3 (Itm2A and Itm2C, respectively), also contain a conserved BRICHOS domain. Whether BRICHOS is secreted in these proteins remains to be verified. The secretion of the complete Bri2 BRICHOS domain strongly suggests that this domain may have a physiological function within the extracellular space and probably even far away from its producing cell. Moreover, in analogy to Notch signaling, one may expect a receptor/ligand interaction inducing shedding and intramembrane proteolysis (46). Interestingly, proteolytic processing of Notch and Bri2 share some remarkable similarities. Both contain a propeptide that is removed by furin or related proteases (32, 33, 46). Furthermore, in both cases, the ectodomain undergoes shedding via a protease of the ADAM family (46). Finally, both proteins undergo intramembrane proteolysis to produce an ICD (43) and a small secreted peptide (Fig. 6 and Ref. 47).

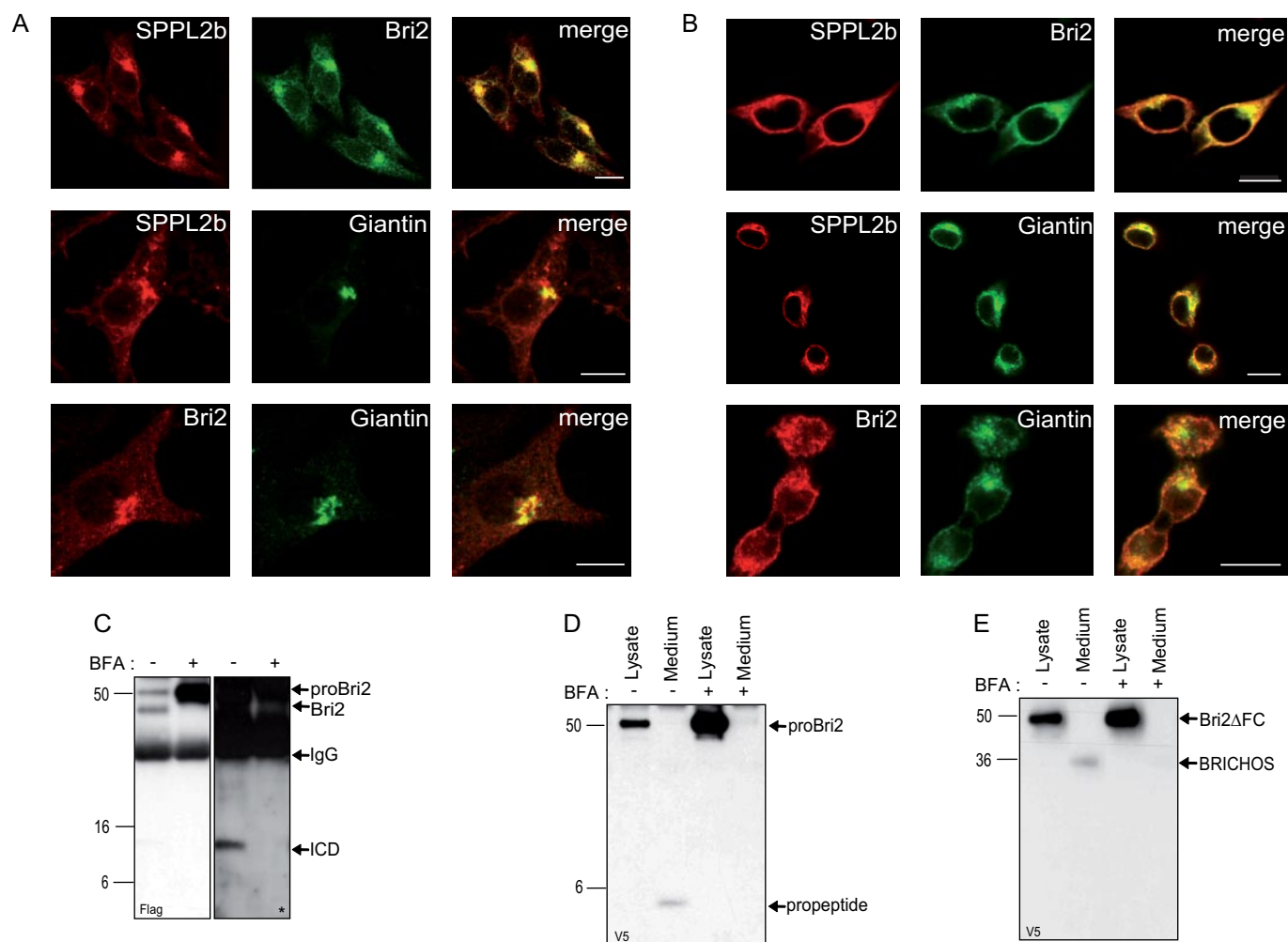


FIGURE 5. Subcellular localization of Bri2 and SPPL2b. *A*, co-localization of Bri2 and SPPL2b. HEK293 cells stably expressing SPPL2b and Bri2 were stained with antibodies against the HA or V5 tag, respectively. Bri2 and SPPL2b are co-localized. SPPL2b as well as Bri2 partially co-stain in the same subcellular structure with the Golgi resident protein Giantin, indicating that SPPL2b and Bri2 interact in the Golgi. *B*, co-localization of Bri2 and SPPL2b in BFA-treated cells. Cells described in *A* were treated with 10 $\mu\text{g}/\mu\text{l}$ BFA overnight and stained as described in *A*. Co-staining of SPPL2b and Bri2 was observed in an ER/Golgi fusion compartment that surrounds the nucleus. The scale bars in *A* and *B* indicate 10 μm . *C*, SPPL2b cleavage was inhibited upon BFA treatment. Cell lysates of cells stably expressing SPPL2b and Bri2 were analyzed for Bri2 fragments using the anti-FLAG antibody. Upon BFA treatment, pro-Bri2 accumulates, whereas Bri2 and Bri2 ICD are no longer produced (asterisk indicates longer blot exposure). *D*, lack of furin cleavage of Bri2 in BFA-treated cells. Cells stably expressing SPPL2b and Bri2 were treated with BFA or carrier only (control) as described in *B*. Upon BFA treatment, pro-Bri2 accumulates (as also shown in *C*). Consistent with the accumulation of pro-Bri2 in cell lysates, no propeptide was detected in either cell lysates or the corresponding conditioned media. *E*, ADAM10 does not cleave Bri2 in BFA-treated cells. Cells stably expressing Bri2 ΔFC were treated as described in the legend Fig. 3C, and the indicated processing products of Bri2 were analyzed. Note that BFA treatment blocks BRICHOS generation in the conditioned medium as well as in the corresponding lysates, indicating that ADAM10 does not cleave Bri2 under these conditions.

Intramembrane proteolysis is again mediated by proteases of the same family, the GXGD proteases. Although these are striking similarities, some obvious differences are observed as well. The substrate proteins, such as Notch and Bri2, have opposite membrane orientation. This is reflected by the corresponding orientations of the catalytically active sites within presenilin and the SPPL2 (1, 15). Furthermore, γ -secretase is a protein complex that absolutely requires four components for its activity (48), whereas SPP and SPPLs apparently do not (29, 37). This is even more surprising if one compares the very similar processing pathways of Notch and Bri2. One of the components of the γ -secretase complex, nicastrin, is required as a substrate-docking site, which accepts only previously shed substrates (49). Shedding also occurs for Bri2, and we could demonstrate that the NTF of Bri2 co-isolates with SPPL2a/SPPL2b. However, in contrast to γ -secretase, which does not bind full-length

substrate (50, 51), we and others (29, 30) found that the full-length substrates (Fas ligand, Bri2, and TNF α) also co-precipitate with SPPL2a/SPPL2b. Apparently, the NTF is preferentially turned over because relatively low levels are bound to proteolytically active SPPL2a/SPPL2b, as compared with the full-length protein (see Fig. 3D and Ref. 29). In contrast, when proteolytically inactive SPPL2a/SPPL2b variants are expressed, higher levels of the NTF co-precipitate (see Fig. 3D and Ref. 29). This suggests that NTFs may be the preferred substrates of SPPL2a/SPPL2b. However, because of the potential lack of an additional cofactor such as nicastrin, less preferred full-length substrates were also bound. One may hypothesize that processing of such longer substrates could apparently be less efficient. Therefore, proteins like nicastrin may have evolved to exclude their binding. In addition to nicastrin, complex stabilization factors and proteins

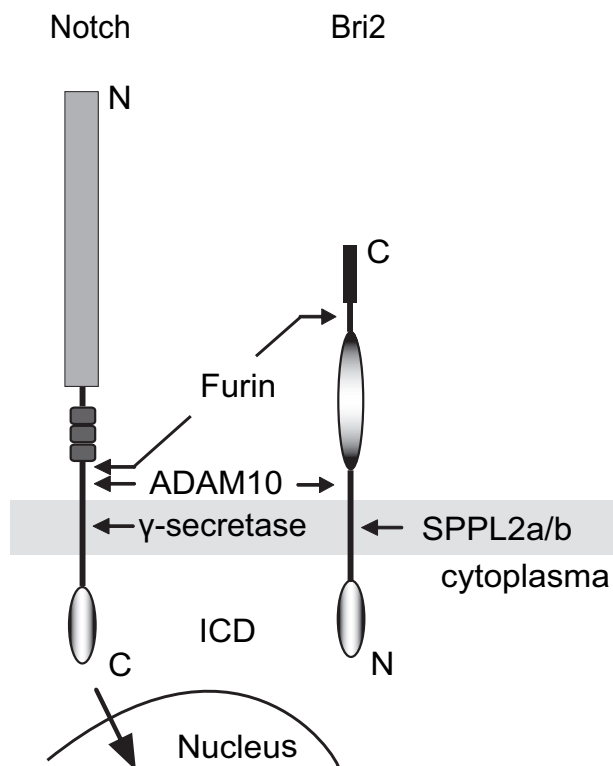


FIGURE 6. **Bri2 processing resembles Notch processing.** Schematic model of Bri2 and Notch processing. Notch and Bri2 are processed by furin, ADAM10, and γ -secretase or SPPL2a/SPPL2b, respectively.

that could transfer the substrate from the docking site to the catalytic center may have evolved. These proteins could be represented by PEN-2 and APH-1 (20).

Another major question is how substrates are selectively recognized by the SPP family members because Fas ligand, TNF α , and Bri2 are preferentially processed by SPPL2a and SPPL2b but not by the highly similar SPP or SPPL3 (29, 30) (Fig. 3C). This may be explained by their differential subcellular localization (26). Although SPP and SPPL3 are restricted to the endoplasmic reticulum, SPPL2a/SPPL2b occur in the Golgi and later secretory compartments such as endosomes/lysosomes (26, 27). Thus the spatial separation of the enzymes and their substrates may contribute to substrate selectivity. However, co-localization by itself is not sufficient for the processing of Bri2 by SPPL2b as demonstrated by the complete inhibition of Bri2 ICD generation upon BFA treatment. Because under these conditions propeptide removal and ectodomain shedding are blocked as well, this suggests three possible explanations for the lack of proteolytic activity of SPPL2b in this compartment: 1) maturation and folding of SPPL2b is incomplete in the ER/Golgi fusion compartment, 2) the pH in this artificial compartment is not optimal for SPPL2b activity, or 3) Bri2 NTF and not Bri2 itself is the preferred substrate for SPPL2b cleavage.

RIP is becoming an increasingly important cellular pathway as the liberated ICDs may have important functions in cellular signaling. The perhaps best understood example is the RIP of Notch, in which the Notch ICD serves as a transcription factor (46). It will be important to determine whether the Bri2 ICD also serves as a part of a signaling cascade. Besides signaling,

intramembrane proteolysis also plays a major role in the removal and subsequent degradation of membrane-retained fragments, which are produced by the initial shedding event (52). A similar membrane proteasome-like function may be taken over by some SPP family members to remove type II-oriented stubs from membranes.

Acknowledgments—We thank Drs. Bruno Martoglio and Christoff Haffner for providing SPP/SPPL cDNAs and Gudula Grammer, Martina Haug-Kröper, and Bärbel Klier for excellent technical assistance.

REFERENCES

1. Weihofen, A., and Martoglio, B. (2003) *Trends Cell Biol.* **13**, 71–78
2. Brown, M. S., Ye, J., Rawson, R. B., and Goldstein, J. L. (2000) *Cell* **100**, 391–398
3. Sakai, J., Duncan, E. A., Rawson, R. B., Hua, X., Brown, M. S., and Goldstein, J. L. (1996) *Cell* **85**, 1037–1046
4. Wang, X., Sato, R., Brown, M. S., Hua, X., and Goldstein, J. L. (1994) *Cell* **77**, 53–62
5. Rawson, R. B., Zelenski, N. G., Nijhawan, D., Ye, J., Sakai, J., Hasan, M. T., Chang, T. Y., Brown, M. S., and Goldstein, J. L. (1997) *Mol. Cell* **1**, 47–57
6. Ye, J., Rawson, R. B., Komuro, R., Chen, X., Dave, U. P., Prywes, R., Brown, M. S., and Goldstein, J. L. (2000) *Mol. Cell* **6**, 1355–1364
7. Lee, J. R., Urban, S., Garvey, C. F., and Freeman, M. (2001) *Cell* **107**, 161–171
8. Urban, S., Lee, J. R., and Freeman, M. (2001) *Cell* **107**, 173–182
9. Foltyni, K., Greenspan, R. J., and Newport, J. W. (2007) *Nat. Neurosci.* **10**, 1160–1167
10. Wang, Y., Zhang, Y., and Ha, Y. (2006) *Nature* **444**, 179–180
11. Wu, Z., Yan, N., Feng, L., Oberstein, A., Yan, H., Baker, R. P., Gu, L., Jeffrey, P. D., Urban, S., and Shi, Y. (2006) *Nat. Struct. Mol. Biol.* **13**, 1084–1091
12. Ben-Shem, A., Fass, D., and Bibi, E. (2007) *Proc. Natl. Acad. Sci. U. S. A.* **104**, 462–466
13. Lemieux, M. J., Fischer, S. J., Cherney, M. M., Bateman, K. S., and James, M. N. (2007) *Proc. Natl. Acad. Sci. U. S. A.* **104**, 750–754
14. Wang, Y., and Ha, Y. (2007) *Proc. Natl. Acad. Sci. U. S. A.* **104**, 2098–2102
15. Weihofen, A., Binns, K., Lemberg, M. K., Ashman, K., and Martoglio, B. (2002) *Science* **296**, 2215–2218
16. Ponting, C. P., Hutton, M., Nyborg, A., Baker, M., Jansen, K., and Golde, T. E. (2002) *Hum. Mol. Genet.* **11**, 1037–1044
17. Grigorenko, A. P., Moliaka, Y. K., Korovaitseva, G. I., and Rogae, E. I. (2002) *Biochemistry (Mosc.)* **67**, 826–835
18. Haass, C., and Steiner, H. (2002) *Trends Cell Biol.* **12**, 556–562
19. LaPointe, C. F., and Taylor, R. K. (2000) *J. Biol. Chem.* **275**, 1502–1510
20. Haass, C. (2004) *EMBO J.* **23**, 483–488
21. Wolfe, M. S., Xia, W., Ostaszewski, B. L., Diehl, T. S., Kimberly, W. T., and Selkoe, D. J. (1999) *Nature* **398**, 513–517
22. Steiner, H., Kostka, M., Romig, H., Basset, G., Pesold, B., Hardy, J., Capell, A., Meyn, L., Grim, M. G., Baumeister, R., Fechteler, K., and Haass, C. (2000) *Nat. Cell Biol.* **2**, 848–851
23. Mumm, J. S., and Kopan, R. (2000) *Dev. Biol.* **228**, 151–165
24. Bentahir, M., Nyabi, O., Verhamme, J., Tolia, A., Horre, K., Wiltfang, J., Esselmann, H., and De Strooper, B. (2006) *J. Neurochem.* **96**, 732–742
25. Okochi, M., Steiner, H., Fukumori, A., Tanii, H., Tomita, T., Tanaka, T., Iwatsubo, T., Kudo, T., Takeda, M., and Haass, C. (2002) *EMBO J.* **21**, 5408–5416
26. Krawitz, P., Haffner, C., Fluhrer, R., Steiner, H., Schmid, B., and Haass, C. (2005) *J. Biol. Chem.* **280**, 39515–39523
27. Friedmann, E., Hauben, E., Maylandt, K., Schleeger, S., Vreugde, S., Lichtenthaler, S. F., Kuhn, P. H., Staufer, D., Rovelli, G., and Martoglio, B. (2006) *Nat. Cell Biol.* **8**, 843–848
28. Loureiro, J., Lilley, B. N., Spooner, E., Noriega, V., Tortorella, D., and Ploegh, H. L. (2006) *Nature* **441**, 894–897
29. Fluhrer, R., Grammer, G., Israel, L., Condron, M. M., Haffner, C., Fried-

- mann, E., Bohland, C., Imhof, A., Martoglio, B., Teplow, D. B., and Haass, C. (2006) *Nat. Cell Biol.* **8**, 894–896
30. Kirkin, V., Cahuzac, N., Guardiola-Serrano, F., Huault, S., Luckerath, K., Friedmann, E., Novac, N., Wels, W. S., Martoglio, B., Hueber, A. O., and Zornig, M. (2007) *Cell Death Differ.* **14**, 1678–1687
31. Vidal, R., Frangione, B., Rostagno, A., Mead, S., Revesz, T., Plant, G., and Ghiso, J. (1999) *Nature* **399**, 776–781
32. Kim, S. H., Creemers, J. W., Chu, S., Thinakaran, G., and Sisodia, S. S. (2002) *J. Biol. Chem.* **277**, 1872–1877
33. Kim, S. H., Wang, R., Gordon, D. J., Bass, J., Steiner, D. F., Lynn, D. G., Thinakaran, G., Meredith, S. C., and Sisodia, S. S. (1999) *Nat. Neurosci.* **2**, 984–988
34. Vidal, R., Revesz, T., Rostagno, A., Kim, E., Holton, J. L., Bek, T., Bojsen-Moller, M., Braendgaard, H., Plant, G., Ghiso, J., and Frangione, B. (2000) *Proc. Natl. Acad. Sci. U. S. A.* **97**, 4920–4925
35. Plant, G. T., Revesz, T., Barnard, R. O., Harding, A. E., and Gautier-Smith, P. C. (1990) *Brain* **113**, 721–747
36. Kaether, C., Capell, A., Edbauer, D., Winkler, E., Novak, B., Steiner, H., and Haass, C. (2004) *EMBO J.* **23**, 4738–4748
37. Weihofen, A., Lemberg, M. K., Ploegh, H. L., Bogoy, M., and Martoglio, B. (2000) *J. Biol. Chem.* **275**, 30951–30956
38. Dovey, H. F., John, V., Anderson, J. P., Chen, L. Z., de Saint Andrieu, P., Fang, L. Y., Freedman, S. B., Folmer, B., Goldbach, E., Holsztynska, E. J., Hu, K. L., Johnson-Wood, K. L., Kennedy, S. L., Kholodenko, D., Knops, J. E., Latimer, L. H., Lee, M., Liao, Z., Lieberburg, I. M., Motter, R. N., Mutter, L. C., Nietz, J., Quinn, K. P., Sacchi, K. L., Seubert, P. A., Shopp, G. M., Thorsett, E. D., Tung, J. S., Wu, J., Yang, S., Yin, C. T., Schenk, D. B., May, P. C., Altstiel, L. D., Bender, M. H., Boggs, L. N., Britton, T. C., Clemens, J. C., Czilli, D. L., Dieckman-McGinty, D. K., Droste, J. J., Fuson, K. S., Gitter, B. D., Hyslop, P. A., Johnstone, E. M., Li, W. Y., Little, S. P., Mabry, T. E., Miller, F. D., and Audia, J. E. (2001) *J. Neurochem.* **76**, 173–181
39. Hundhausen, C., Misztela, D., Berkhout, T. A., Broadway, N., Saftig, P., Reiss, K., Hartmann, D., Fahrenholz, F., Postina, R., Matthews, V., Kallen, K. J., Rose-John, S., and Ludwig, A. (2003) *Blood* **102**, 1186–1195
40. Choi, S. I., Vidal, R., Frangione, B., and Levy, E. (2004) *FASEB J.* **18**, 373–375
41. Arribas, J., Coodly, L., Vollmer, P., Kishimoto, T. K., Rose-John, S., and Massague, J. (1996) *J. Biol. Chem.* **271**, 11376–11382
42. De Strooper, B., Saftig, P., Craessaerts, K., Vanderstichele, H., Guhde, G., Annaert, W., Von Figura, K., and Van Leuven, F. (1998) *Nature* **391**, 387–390
43. De Strooper, B., Annaert, W., Cupers, P., Saftig, P., Craessaerts, K., Mumm, J. S., Schroeter, E. H., Schrijvers, V., Wolfe, M. S., Ray, W. J., Goate, A., and Kopan, R. (1999) *Nature* **398**, 518–522
44. Klausner, R. D., Donaldson, J. G., and Lippincott-Schwartz, J. (1992) *J. Cell Biol.* **116**, 1071–1080
45. Sanchez-Pulido, L., Devos, D., and Valencia, A. (2002) *Trends Biochem. Sci.* **27**, 329–332
46. Selkoe, D., and Kopan, R. (2003) *Annu. Rev. Neurosci.* **26**, 565–597
47. Okochi, M., Steiner, H., Fukumori, A., Tanii, H., Tomita, T., Tanaka, T., Iwatsubo, T., Kudo, T., Takeda, M., and Haass, C. (2002) *EMBO J.* **21**, 5408–5416
48. Edbauer, D., Winkler, E., Regula, J. T., Pesold, B., Steiner, H., and Haass, C. (2003) *Nat. Cell Biol.* **5**, 486–488
49. Shah, S., Lee, S. F., Tabuchi, K., Hao, Y. H., Yu, C., LaPlant, Q., Ball, H., Dann, C. E., III, Sudhof, T., and Yu, G. (2005) *Cell* **122**, 435–447
50. Thinakaran, G., Regard, J. B., Bouton, C. M., Harris, C. L., Price, D. L., Borchelt, D. R., and Sisodia, S. S. (1998) *Neurobiol. Dis.* **4**, 438–453
51. Esler, W. P., Kimberly, W. T., Ostaszewski, B. L., Ye, W., Diehl, T. S., Selkoe, D. J., and Wolfe, M. S. (2002) *Proc. Natl. Acad. Sci. U. S. A.* **99**, 2720–2725
52. Kopan, R., and Ilgan, M. X. (2004) *Nat. Rev. Mol. Cell Biol.* **5**, 499–504

Regulated Intramembrane Proteolysis of Bri2 (Itm2b) by ADAM10 and SPPL2a/SPPL2b

Lucas Martin, Regina Fluhrer, Karina Reiss, Elisabeth Kremmer, Paul Saftig and Christian Haass

J. Biol. Chem. 2008, 283:1644-1652.

doi: 10.1074/jbc.M706661200 originally published online October 25, 2007

Access the most updated version of this article at doi: [10.1074/jbc.M706661200](https://doi.org/10.1074/jbc.M706661200)

Alerts:

- [When this article is cited](#)
- [When a correction for this article is posted](#)

[Click here](#) to choose from all of JBC's e-mail alerts

This article cites 52 references, 17 of which can be accessed free at <http://www.jbc.org/content/283/3/1644.full.html#ref-list-1>